

SMOOTHED PARTICLE HYDRODYNAMICS APPLIED TO THE SIMULATION OF LOW REYNOLDS NUMBER FLOWS

Coelho, J. G., josegustavo@unb.br

Oliveira, T. F., taygoara@unb.br

Brasil, A. C. P., brasiljr@unb.br

Department of Mechanical Engineering, University of Brasilia (UnB)

Maruzewski, P., pierre.maruzewski@epfl.ch

Ecole Polytechnique federale de Lausanne- EPFL, Lausanne, Switzerland

Abstract. *In this work we use the Smoothed Particle Hydrodynamics methodology (SPH) to simulate incompressible viscous flows of Newtonian fluids. The SPH is a meshfree Lagrangian method which simulates the flow like a set of moving fluid particles that interact one with others by hydrodynamics forces. The forces acting on each particle are evaluated using a spatial filtering process, taken over a certain region in the neighborhood of the particle which is defined by a smoothing length, h . The filter kernel function and the ratio of the mean spatial displacement of the particles, and the smoothing length, h , are both of central importance for the accuracy of this methodology. A study of the relative importance of this parameters and also of the boundary condition scheme and pressure constitutive model are performed in a context of low Reynolds numbers flow. The model is validated by comparison with analytical solution of the Stokes equations. Additionally, the cases $Re = 1$ and $Re = 100$ are simulated. Good agreement of the results of the simulations and the reference theoretical data was observed.*

Keywords: *smoothed particle hydrodynamics, mesh free methods, low Reynolds number flow.*

1. INTRODUCTION

Smoothed Particle Hydrodynamics (SPH) is a meshfree lagrangean method which may be used to simulate a variety of physical phenomena. Originally, SPH was designed by Monaghan [13] to simulate galaxy dynamics. Currently, it is employed to simulate continuum phenomena like elastic materials behavior [17], fluid dynamics [15], [7], explosions [11] and non-Newtonian fluid flows [19]. In the case of fluid flow simulations, the SPH method look for numerical solutions of the equations of fluid dynamics by replacing the material by a set of discrete lagrangean particles or control points. In this sense, each control point represents a material particle which is allowed to interact with its neighborhood. This interaction occurs by pairwise systems of hydrodynamics forces acting between the particles. The computation of this forces are made by using some spatial average procedure which favors the nearest neighbors. Mathematically, it can be reached by using spatial interpolation functions (kernels) to evaluate the properties of a particular material point in the flow. More details about this procedure are given in sections above.

One of the most important characteristics of the SPH is its adaptive nature. SPH is meshfree method and doesn't need no connected mesh. Actually, in order to find the hydrodynamic properties (velocity, pressure, density, ...) of a particle we only need to know the state of the neighbors particles. So, the problem is solved always by a local analysis and there are no rigid restriction to the spatial distribution of particles over the domain. Those features leads a very natural treatment of free surface, very large deformations or moving boundaries problems [11]. The price to be paid for this feature is the determination the neighbor particles at each new configuration (or each time step of the time evolution). In the case of incompressible flows, an additional difficulty appears from the determination of the pressure field. The SPH formulation is designed to treat all the quantities of the problem by an explicit approach. In this sense, even in incompressible fluid flows, a state equation for the pressure is need in order to keep the solution local and to avoid the global determination of the pressure field by coupling algorithms like the ones of the SIMPLE family.

Nowadays, there are a relatively wide bibliography about SPH. Some featured work are [16] which suggest some variations of state equations for liquid fluid flows simulations in order to accommodate the low Reynolds number condition. Monaghan, [15], [12], make a wide revision about the subject showing the recent advances in the field and the main issues to be studied and developed. A deep analysis about the importance of the kernel function was made by Hongbin and Xin, [8].

The goal of this work is to apply the SPH method to solve incompressible Newtonian fluid flows at low Reynolds numbers. This work is a first step in the definition of a meshfree methodology to study flows over solid boundaries which are moving and interacting with the flow (fluid-structure interactions). A computational code was developed based on a typical SPH model for incompressible flows. The accuracy of the model is evaluated by comparison of the velocity fields with results obtained by constructed solutions for the Stokes equations, in the case of $Re \ll 1$. For more moderate Reynolds numbers, experimental results are used like reference to our simulations.

2. GOVERNING EQUATIONS

The principle of mass and momentum conservation for Newtonian fluid flows can be written in the Lagrangean form like

$$\frac{D\rho}{Dt} = -\rho \nabla \cdot \mathbf{u} \quad (1)$$

$$\frac{D\mathbf{u}}{Dt} = -\frac{1}{\rho} \nabla P + \frac{1}{\rho} \nabla \cdot \boldsymbol{\tau} + \mathbf{F} \quad (2)$$

where ρ is the density of the fluid, \mathbf{u} the velocity field (which is the velocity of the material particle), P the pressure field, \mathbf{F} an external force by unity of mass and $\boldsymbol{\tau}$ is the deviatoric part of the stress tensor of the fluid. The nabla operator, ∇ , have the conventional meaning and the material derivative is defined by $D/Dt = \partial/\partial t + \mathbf{u} \cdot \nabla$. We employ the compressible form of the continuity equation (1) because de SPH methodology was designed for treat all quantities explicitly, [11]. In such a case, even for incompressible flows we need a constitutive equation for the pressure field, in order to close the problem in the mathematical point of view. In practice, it means that even for incompressible flow, we have a level of artificial compressibility, which must be carefully tracked along the simulations. In general, for high Reynolds numbers flows, the equation

$$P = \frac{\rho_0 c^2}{\gamma} \left[\left(\frac{\rho}{\rho_0} \right)^\gamma - 1 \right] \quad (3)$$

where $\gamma = 7$, gives a good approximation of the pressure field for liquids, subjected to small density variations ([1], [12]). By using these state equation for the pressure typically we find a sound velocity throughout the medium, c , about ten times the maximum velocity in the domain. For low Reynolds number flow, Morris (1997), [16], has proposed a linear relation between the pressure, P , and the density, ρ , in the form

$$P = c^2 \rho. \quad (4)$$

This approach potentially leads to great variation of pressure, depending of the sound speed in the medium, c . Morris (1997), [16], recommends to set the value of c in such a way that the density variation keep below 3%. By using some scaling arguments, Liu (2003), [11] shows that an initial approximation for c may be obtained by

$$c^2 \approx \max \left(\frac{\mathbf{U}_0}{\delta_*}, \frac{\nu \mathbf{U}_0}{L \delta_*}, \frac{\mathbf{F}L}{\delta_*} \right) \quad (5)$$

where $\delta_* = \frac{\Delta \rho}{\rho_0}$, ρ_0 is a reference density, \mathbf{U}_0 a characteristic velocity and L a characteristic length. But these estimation must be taken like an initial guess only. The final value of c must be carefully adjusted in order to keep $\Delta \rho / \rho_0 < 0.03$.

3. SPH FORMULATIONS

3.1 Core SPH

In SPH formulation the fluid is represented by a set of discrete point particles. Each particle have physical properties like density, mass, volume, pressure and velocity. The only invariant parameter is the mass of the particle. All other quantities are allow to vary during the temporal evolution. The particle properties actually represents a spatial average over a certain portion of the domain. Considering a generic property α (which can be any scalar, vectorial or tensorial quantity) it value for a particle in a specific position \mathbf{r} is given by

$$\alpha(\mathbf{r}) = \int_{\Omega} \alpha(\mathbf{r}') W(\mathbf{r} - \mathbf{r}') d\mathbf{r}', \quad (6)$$

where W is an interpolation, or kernel, function, which obey all properties of a typical probability density function, [10], and Ω is the domain. In practice, this integration is taken only over a portion of the domain, which defines the neighborhood of the particle. In this work we use the cubic spline kernel, defined by

$$W(s) = \begin{cases} 1 - \frac{3s^2}{2} + \frac{3s^3}{4} & \text{if } 0 \leq s < 1; \\ \frac{2-s^3}{4} & \text{if } 1 \leq s < 2; \\ 0 & \text{if } s \geq 2; \end{cases} \quad (7)$$

where $s = \frac{r}{h}$, h is the so called smoothed length and $r = \sqrt{(\mathbf{r} - \mathbf{r}') \cdot (\mathbf{r} - \mathbf{r}')}$. The integration in the equation (7) actually is approximated by a summation over the discrete particles in the neighborhood of the particle. By this way, considering a particle a , in the position \mathbf{r}_a , equation (6) reduces to

$$\alpha(\mathbf{r}_a) \approx \sum_b \frac{m_b}{\rho_b} \alpha_b W(r_{ab}) \quad (8)$$

where b indicate that the summation is taken over the neighborhood of the particle, m is the mass and r_{ab} is the distance between the particle a and the particle b .

In order to write the governing equations in the discrete form in the SPH way, we must to know how the convolution defined in the equation (6) operate over the differential operators in the governing equations. It is possible to show [11] that the gradient of a quantity α can be approximated by

$$\nabla\alpha(\mathbf{r}_a) \approx \sum_b \frac{m_b}{\rho_b} \alpha_b \nabla_a W(r_{ab}) \quad (9)$$

where $\nabla_a W(r_{ab})$ denotes the gradient of the kernel function in relation to the particle a . Others forms for the gradient can be derived by using the vectorial identities (10) and (11), bellow

$$\nabla\alpha = \rho \left[\nabla \left(\frac{\alpha}{\rho} \right) + \frac{\alpha}{\rho^2} \nabla\rho \right], \quad (10)$$

$$\nabla\alpha = \frac{1}{\rho} (\nabla(\rho\alpha) - \alpha\nabla\rho). \quad (11)$$

Combining equations 9 and 10 one can show that

$$\nabla\alpha(\mathbf{r}_a) \approx \rho_a \sum_b m_b \left(\frac{\alpha_a}{\rho_a^2} + \frac{\alpha_b}{\rho_b^2} \right) \nabla_a W(r_{ab}). \quad (12)$$

Furthermore, if we combine equations 9 and 11, one obtains

$$\nabla\alpha(\mathbf{r}_a) \approx \frac{1}{\rho_a} \sum_b m_b (\alpha_b - \alpha_a) \nabla_a W(r_{ab}). \quad (13)$$

The important distinctive difference between the approximations for the gradient given by equations (12) and (13) is that (12) is symmetric and (13) is anti-symmetric to change in the positions of the particles indices a and b [9]. Similar formula may be derived to the divergent operator. Examples of utilization of gradient and divergent SPH operators in the governing equations are

$$\nabla P_a \approx \rho_a \sum_b m_b \left(\frac{P_b}{\rho_b^2} + \frac{P_a}{\rho_a^2} \right) \nabla_a W(r_{ab}) \quad (14)$$

and

$$\nabla \cdot \mathbf{u}_a \approx -\frac{1}{\rho_a} \sum_b m_b \mathbf{u}_{ab} \cdot \nabla_a W(r_{ab}) \quad (15)$$

where $\mathbf{u}_{ab} = \mathbf{u}_a - \mathbf{u}_b$. Other way for the approximations for the gradient and divergent operator are developed by Monaghan (1992), [13].

Most implementations of SPH uses an artificial viscosity to simulate the viscous effect. In this sense, the momentum equations (2) takes the form

$$\frac{D\mathbf{u}_a}{Dt} = -\sum_b m_b \left(\frac{P_a}{\rho_a^2} + \frac{P_b}{\rho_b^2} + \Pi_{ab} \right) \nabla_a W(r_{ab}) + \mathbf{F}_a \quad (16)$$

where Π_{ab} is the viscous contribution and \mathbf{F}_a is the body force evaluated at the particle a . The original expression for Π_{ab} was empirically design to permit the stabilization of shock simulations [13], and typically doesn't work well for the estimation of the velocity profile in low, or even moderate, Reynolds number flows. Several others approximations can be found in the literature ([9], [11], [12]). In this work, we uses the artificial viscosity proposed by Morris *et. al.* (1997) [16] where the viscous forces are calculated in a separated summation and the discrete momentum equations becomes

$$\frac{D\mathbf{u}_a}{Dt} = -\sum_b m_b \left(\frac{P_a}{\rho_a^2} + \frac{P_b}{\rho_b^2} \right) \nabla_a W(r_{ab}) + \sum_b \frac{m_b(\mu_a + \mu_b)\mathbf{u}_{ab}}{\rho_a\rho_b} \left(\frac{1}{r_{ab}} \frac{\partial W_{ab}}{\partial r_a} \right) + \mathbf{F}_a \quad (17)$$

The continuity equation in the SPH discrete form becomes

$$\frac{D\rho_a}{Dt} = \sum_b m_b \mathbf{u}_{ab} \cdot \nabla_a W_{ab}. \quad (18)$$

The equations (17) and (18) are integrated in time by an Euler method restricted to the condition

$$\Delta t = \min \left\{ 0.25 \frac{h}{c}, 0.25 \min_a \sqrt{\frac{h}{f_a}}, 0.125 \min_a \frac{h^2}{\nu} \right\} \quad (19)$$

3.2 Boundary conditions

The application of the boundary conditions in SPH has been subject of several developments in the last few years. A very popular method consist in to set a repulsive force in particles just over the solid walls of the domain. Some molecular models, like Leonard-Jones like models [11], was used to prevent penetration of inter particles through the boundaries. So, the particles at the walls interact with their neighbors by a force given by

$$FP_{ab} = \begin{cases} D \left[\left(\frac{r_o}{r_{ab}} \right)^1 2 - \left(\frac{r_o}{r_{ab}} \right)^4 \right] \frac{x_{ab}}{r_{ab}^2} & \text{if } \frac{r_o}{r_{ab}} \leq 1; \\ 0 & \text{if } \frac{r_o}{r_{ab}} > 1; \end{cases} \quad (20)$$

The constant D is of the magnitude of the square of the maximum velocity in the domain. The distance r_o is approximately equal to the initial separation between the particles. Both these parameters are of crucial importance to stability of the boundary condition. If D is too big, particles which becomes so closed to the wall may be violently putted back, causing oscillations and eventually, the crashing of the simulation. In the other hand, small values of D may allow the particles to pass through the walls and to be putted out of the domain [11]. Other options for boundary condition implementation are the so called ghosts (or virtual) particles created with symmetric properties in relation to the real ones, inside the domain [16], [20]. Recent development was made by Crespo (2007) [2] in the treatment of fixed wall particles. In the present work, we employ the standard formulation given by equation (20).

4. CONSTRUCTED SOLUTIONS

In the present work, a C++ computational code was developed in order to simulate incompressible flows in closed domains and in low Reynolds numbers regimes. Like a first benchmark, we employ some constructed solution of the Stokes equations. We set Re to be much less than the unity, in a such way that the governing equation can be well approximated by the Stokes equation, given by,

$$\mathbf{F} = \frac{1}{\rho} \nabla P - \nu \nabla^2 \mathbf{u}, \quad (21)$$

$$\nabla \cdot \mathbf{u} = 0. \quad (22)$$

where the domain is defined by all positions \mathbf{x} such that $\mathbf{x} \in [0, 1] \times [0, 1]$. In other words, the flow domain is a 2D unity square cavity. The flow bind to the solid wall providing a non-slip boundary condition. An analytic solution of the equations (21) and (22) is obtained by choosing a velocity field $\mathbf{u} = (u_1, u_2)$ which respect the continuity equation. We choose a polynomial form of u_1 and u_2 given by

$$u_1 = x_1^2 (1 - x_1)^2 (2x_2 - 6x_2^2 + 4x_2^3), \quad (23)$$

$$u_2 = -x_2^2 (1 - x_2)^2 (2x_1 - 6x_1^2 + 4x_1^3). \quad (24)$$

It can be observed that the velocity field given by equations (23) and (23) keep the non-slip condition over the edges of the square domain. The pressure is set to constant throughout the flow field. The velocity field is replaced into equation (21) and the body force $\mathbf{F} = (F_1, F_2)$ is then determined, resulting

$$F_1 = (-24x_2 + 12)x_1^4 + (48x_2 - 24)x_1^3 + (-48x_2^3 + 72x_2^2 - 48x_2 + 12)x_1^2 + (48x_2^3 - 72x_2^2 + 24x_2 - 2)x_1 + (1 - 4x_2 + 12x_2^2 - 8x_2^3), \quad (25)$$

$$F_2 = (48x_2^2 - 48x_2 + 8)x_1^3 + (-72x_2^2 + 72x_2 - 12)x_1^2 + (24x_2^4 - 48x_2^3 + 48x_2^2 - 24x_2 + 4)x_1 + (-12x_2^2 + 12x_2^3 - 12x_2^4). \quad (26)$$

So, in this way, the velocity field given by (23) and (24), the body force given by (25) and (26) and a constant pressure field are an analytic solution of the Stokes equation in the square domain $[0, 1] \times [0, 1]$.

In order to use these solution as a benchmark to the computational code, we programm the body force in the equation (17) in such manner to obey the expressions (25) and (26). We expect to recover a velocity field equal to given by (23) and (24).

4.1 Results and discussion

We perform a first simulation where $Re = 10^{-6}$. We define the Reynolds number based on the maximum velocity throughout the domain (which we known previously) and also in the unitary length of the square edge. We use 1600 intern

fluid particles uniformly spaced at the beginning of the simulation. It was necessary 320 particles to establish the walls. The smoothing length, h , is a central parameter in SPH simulations. Large values of h favors a good spatial average, because the influence radio of the kernel function becomes wider and a more particles are used in the mean processes. In other hand, to keep the local character of the model, the neighborhood should be narrow. Large values for h also tends to impose some over diffusion. In this work, we made a sensitive analysis in which we vary h and track the mean square deviation of the velocity components of the particles, defined by

$$\epsilon = \frac{1}{n} \sum_{i=1}^n (u_{sp} - u_a)^2 \tag{27}$$

where n is he number of particle in the domain, u_{sph} is the simulation result, u_a is the analytical value for the u component of the velocity vector. Figure (1) shows the velocity vectors of a simulation with $h = 1.1\Delta x_o$, where Δx_o is the initial separation between the particles. Figures (2) and (3) shows the velocity profile at the horizontal central line compared

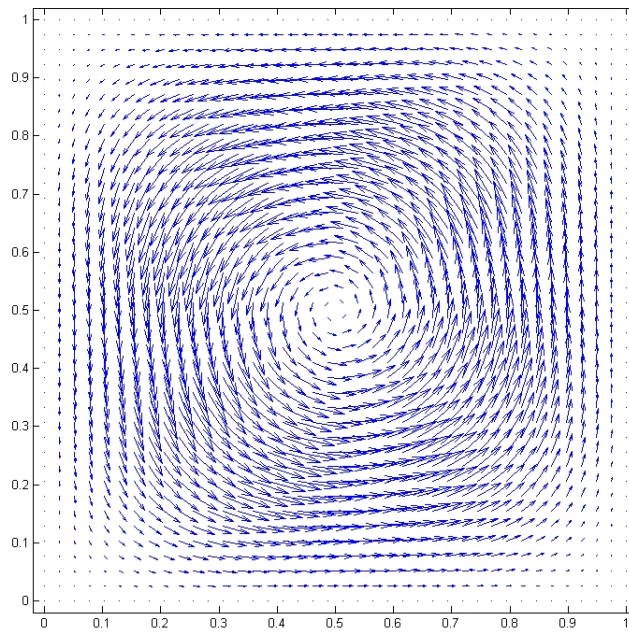


Figure 1. Velocity vectors for $h = 1.1\Delta x_o$.

with the analytical solution. It is possible to observe that for $h = 1.3\Delta x_o$ the results qualitatively agree more closely. The table (1) shows the results for the mean square deviation, ϵ , like a function of h . We can observe that ϵ reach a

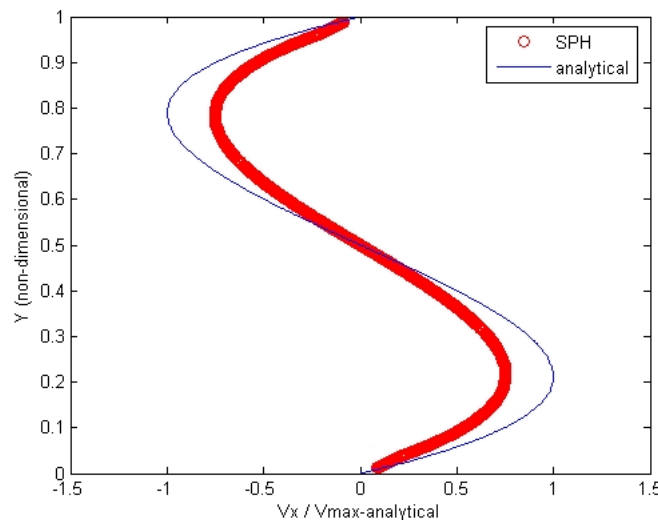


Figure 2. Velocity profile at the horizontal central line for $h = 1.1\Delta x_o$.

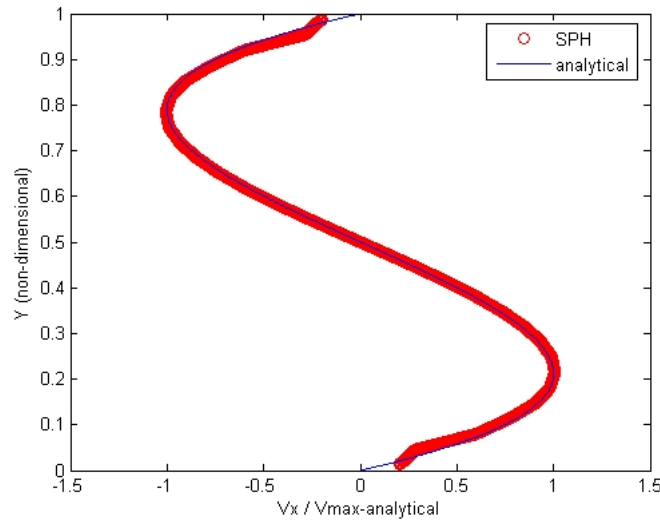


Figure 3. Velocity profile at the horizontal central line for $h = 1.3\Delta x_o$

Table 1. Mean square and maximum deviation as a function of the smoothing length for 1600 particles.

$h/\Delta x_o$	ϵ	maximum deviation
1.1	0.03430	0.0630
1.2	0.03100	0.0567
1.5	0.00380	0.0115
1.6	0.00048	0.0110
1.7	0.00590	0.0130
2.0	0.07210	0.1518

minimum approximately for $h = 1.6\Delta x_o$. The same behavior repeats for the maximum deviation between the analytical and numerical solutions.

Monaghan (2005), [12], stress the importance of the number of particles for SPH simulation. Actually, in a wider sense, discrete methods must to preserve an invariance in relation of the number of particles. In order to infer how the present model is sensible to the number of particles, we run simulations with 400, 900, 1600, 2500 and 3600 particles. In each case, we look for the optimum smoothing length too. For 400 particles we cannot to stabilize the simulation. For 900 particles we find out that the optimum smoothing length is different that we have found for 1600 particles, like can be seen in the table (2). figure (4) shows ϵ as a function of the number of particles. We can observe that ϵ appears to

Table 2. Mean square and maximum deviation as a function of the smoothing length for 900 particles.

$h/\Delta x_o$	ϵ	maximum deviation
1.2	0.0045	0.0157
1.3	0.0011	0.0144
1.6	0.1078	0.2249
2.7	10.517	21.509

approximate to a plateau for large number of particles. Probably, the residual which still remains came from the temporal integration. Its is important to alert that for each new value of n (number of particles) we proceed with a new optimization procedure. In these sense, we plot the optimum smoothing length as a function of the number of particles. In the Figure (5) we can observe that these relation is very close to linear in the interval we has studied.

5. SHEAR DRIVEN CAVITY FLOW

The other test we made with the numerical model was a simulation of the shear driven cavity flow. It is a classic benchmark used as reference for numerical studies of low and moderate Reynolds number flows. In the present case, the flow domain is a 2D square box with length of the edge $L = 10^{-3}m$. The upper wall of the cavity moves from left to right with constant velocity $U = 10^{-2}m/s$. We change the Reynolds number, $Re = UL/\nu$, by varying the kinematic viscosity, ν . The most important difference in the present flow in relation to the previous one is the fact that here the

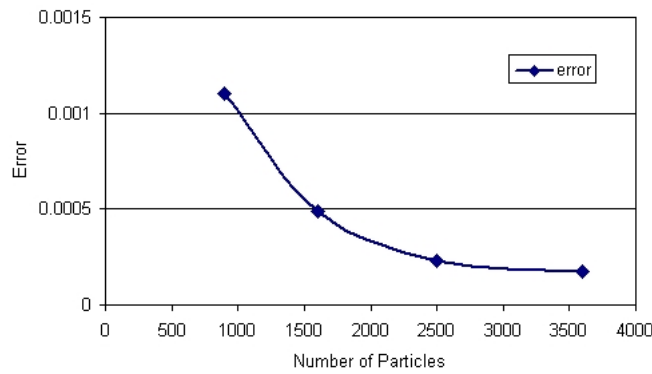


Figure 4. Mean square deviation as a function of the number of particles.

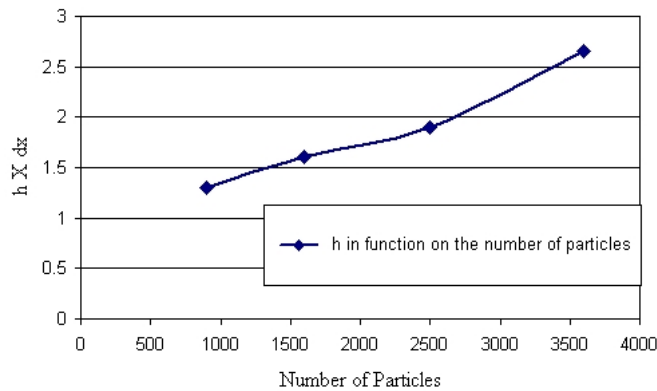


Figure 5. Optimum smoothing length as a function of number of fluid particles.

driven force comes from the shear stress term, while in the other case was a body force. To simulate the constant velocity plate at the top of the cavity, we create a line of particles which velocity is always equal to U but don't are allowed to change its positions. We perform two different simulations for $Re = 1$ and $Re = 100$, respectively. Experimental and numerical data available in the literature was employed in quantitative comparisons.

5.0.1 $Re = 1$

In this case, we use 1600 fluid particles and 320 wall particles. The smoothing length, h , is equal to the initial separation between the particles. We compare our results with numerical data from finite element simulations obtained by Liu (2003), [11]. Figure (6) shows the velocity vectors after the steady state. For quantitative validation, we extract

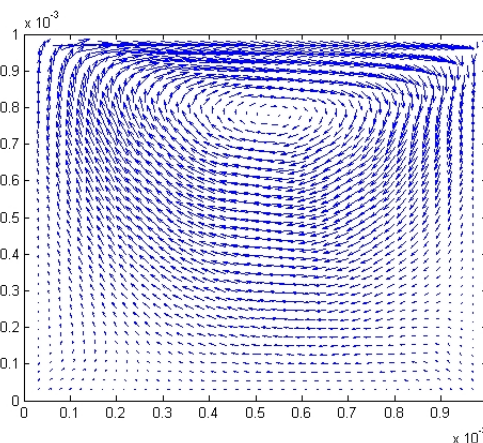


Figure 6. Shear-driven cavity flow. Velocity vectors for $Re = 1$.

the profile of horizontal component of the velocity vector at the central vertical line in the cavity and compare with the

reference data. This comparison is shown in Figure (7). We can observe a good agreement between results.

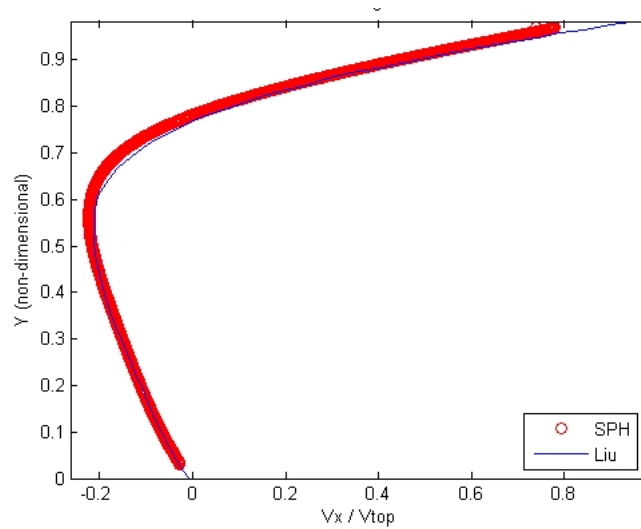


Figure 7. Horizontal component of the velocity at the central line in the cavity for $Re = 1$. Red thick line is SPH results and black thin line is the numerical data from Liu (2003)

5.0.2 $Re = 100$

In this case, we use 6400 fluid particles and 320 wall particles. The smoothing length, is $h = 1.3\Delta x_o$. We compare our results with experimental data obtained by Ghia (1982), [5]. Figure (6) shows the velocity vectors after the steady

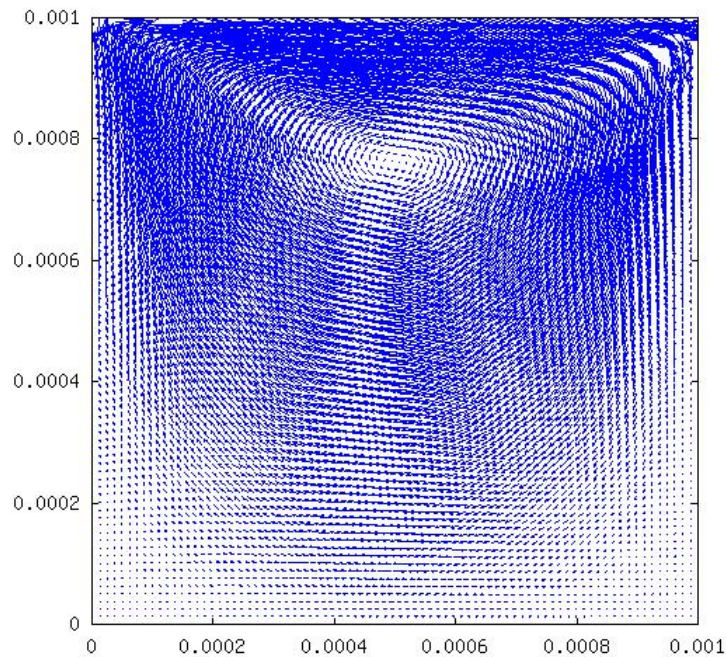


Figure 8. Shear-driven cavity flow. Velocity vectors for $Re = 100$.

state. We can observe a numerical oscillation at the upper right corner. One more time, we extract the profile of horizontal component of the velocity vector at the central vertical line in the cavity and compare with the experimental data. This comparison is shown in Figure (7). We can observe a good agreement between results in the bottom portion of the plot, but as we approximate to the moving plate the results turns away one each other. It is clear that the numerical oscillation has negative effects over the results of the simulation

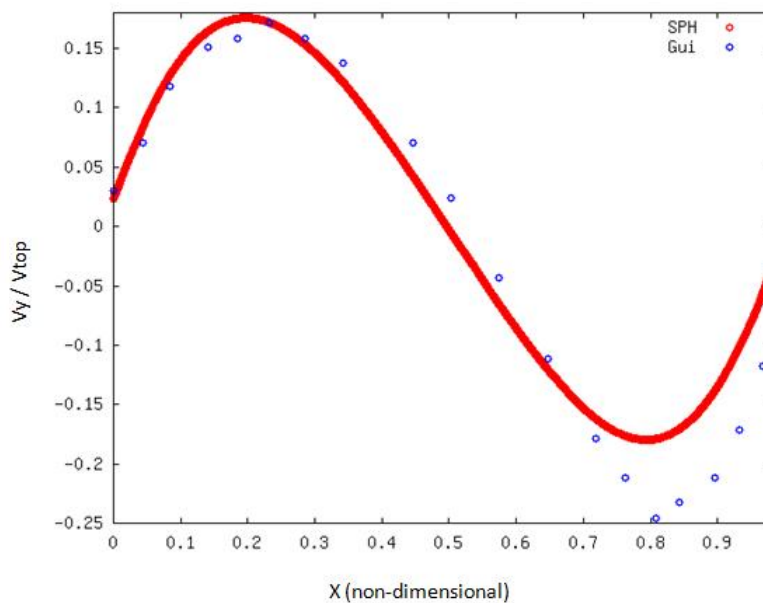


Figure 9. Horizontal component of the velocity at the central line in the cavity for $Re = 100$. Red thick line is SPH results and black thin line is the experimental data from Ghia (1982).

6. CONCLUSIONS

A SPH numerical code for the simulation of low Reynolds number flows was implemented. Initial tests were carried out by comparing numerical results with constructed analytical solutions of the Stokes equations. We study the influence of the smoothing length, h , on the accuracy of the model. We found that the optimal value of h depends on the number of particles, n , inside the domain. An approximately linear relation between h and n . Some additional study on this subject is necessary. The 2D shear driven cavity flow was also simulated and some preliminary comparison with data available in the literature was made. We found a good agreement for $Re = 1$. For $Re = 100$ some numerical emerged from the upper right corner of the cavity. We suspect that the boundary condition scheme doesn't treat well the difficulty associated to this singularity.

7. ACKNOWLEDGEMENTS

This work is supported by the project P&D-4500063744 of the ELETRONORTE S.A.

8. REFERENCES

- Batchelor, G. K., 1967, "An Introduction to Fluid Dynamics", Cambridge Press.
- Crespo A. J. C., Gesteira M. G., Dalrymple R. A., 2007, "Dynamical Boundary Particles in SPH", Spheric-book (2007), 13-14. Madrid, May 23-25, 2007.
- Dalrymple R. A., Rogers B. D., 2005, "Numerical modeling of water waves with the SPH method", Coastal Engineering 53 (2006), 141-147.
- Donea J., Huerta A., 2003, "Finite Elements Methods for Flow Problems", John Wiley e Sons Ltda. Englan, 363p.
- Ghia U., Guia K. N., Shin C. T., 1982, "High-Re Solutions for Incompressible Flow Using the Navier-Stokes Equations and a Multigrid Method", Journal of Computational Physics 48, 387-411 (1982).
- Groenenboom P., 2007, "High-velocity impact simulation by a hybrid SPH-FE method in PAM-SHOCK", Spheric-book (2007), 13-14. Madrid, May 23-25, 2007.
- Hu X. Y., Adams N. A., 2007, "An incompressible multi-phase SPH method", Journal of Computational Physics 227 (2007), 264-278.
- Hongbin J., Xin D., 2005, "On criterios for smoothed particle hydrodynamics kernels in stable field", Journal of Computational Physics 202 (2005), 699-709.
- Lee E. -S., Moulinec C., Xu R., Diouveau D. Laurence D., Stansby P., 2008, "Comparisons of weakly compressible and trully incompressible algorithms for the SPH mesh free particle method", Journal of Computational Physics 227 (2008), 8417 - 8436.
- Libersky L. D., Petschek A. G., Carney T. C. Hipp J. R., Allahdadi F. A., 1993, "High strain Lagrangian Hydrodynamics", Journal Computational Physics 109, 67 (1993).

- Liu G. R., Liu M. B., 2003, "Smoothed Particle Hydrodynamics", Ed. World Scientific Publishing, Singapore, China, 473 P.
- Monaghan J. J., 2005, "Smoothed Particle Hydrodynamics", Institute of Physics Publishing, Reports on Progress in Physics 68 (2005), 1703 - 1759.
- Monaghan J. J., 1992, "Smoothed Particle Hydrodynamics", Annual Review of Astronomy and Astrophysics 30, 543 - 574.
- Monaghan J. J., 2002, "Simulating Free Surface Floes with SPH", Journal of computational Physics, 110, 399-306.
- Monaghan J. J., 2002, "SPH compressible turbulence", Royal Astronomical Society, 335, 843-852.
- Morris J. P., Fox P.J., Zhu Y., 1997, "Modelling Low Reynolds Number Incompressible Flows Using SPH", Journal of Computational Physics 136, 214-226.
- Morris J. P., 2000, "Simulating surface tension with smoothed particle hydrodynamics", International Journal for Numerical Methods in Fluids, 2000; 33, 333-353.
- Panizzo A., Capote T., Marrone S., 2008, "Experiences of SPH with the lid driven cavity problem", Spheric-book (2008), Lausanne, Switzerland, June 04-06, 2008, 74-77.
- Shao Songdong, Lo Edmond Y. M., 2003, "Incompressible SPH method for simulating Newtonian and non-Newtonian flows with a free surface", Advances in Water Resources 26 (2003), 787 - 800.
- Yildiz M., Rook R. A., Suleman A., 2008, "SPH with the multiple boundary tangent method", International Journal for Numerical Methods in Engineering DOI: 10.1002/nme.2458.

9. Responsibility notice

The author(s) is (are) the only responsible for the printed material included in this paper